Approaching Higher Frequencies – Quantitative Evaluation of Air-Coupled UT Transducers

Mario Kiel[1], Ralf Steinhausen[1], Stefan Scheunemann[1], Klaus-V. Jenderka[2]

[1] *Forschungszentrum Ultraschall gGmbH, 06118 Halle (Saale), Germany, Email: ralf.steinhausen@fz-u.de*

[2] *Hochschule Merseburg, FB INW, 06217 Merseburg, Germany, Email: klaus.jenderka@hs-merseburg.de*

Introduction

Real quantitative characterization of airborne ultrasonic waves above 100 kHz still raise challenging questions in research and development. Exemplary, development of new concepts for air-coupled ultrasonic transducers needs objective methods for characterization which are independent of the frequency (broad-band measurements). In deed, an optical approach as used in laser-doppler vibrometers (LDV) or optical microphones (OM) seems to close this given gap.

In this paper we present a direct comparison of both methods applied on characterization of sound field properties of ultrasonic transmitters. The influence of probably resonance effects due to geometric properties will be discussed. The results lead to additional objective characterization opportunities for ultrasonic receivers as well.

Methods

The measurement of acoustic waves is based on the pressure dependence on refractive index of air which leads to a change of speed of light [1, 2]. The laser-doppler vibrometer [3] and the optical microphone [4] apply an interferometric measurement to get access to this relatively small changes of speed of light due to the alterations of air pressure caused by a sound source, here ultrasonic transducers. This change is converted into an analog signal which is processed as well-known A-scans. The method has already been presented in [5] and will not be further discussed. The main issue of this paper will be direct comparison of both methods. In Fig. 1 the different working principles of both methods are depicted. As shown in Fig. 1(a) the laser beam of the LDV is directed through the whole sound field of the transducer almost perpendicular (see remark below) to its acoustic axis. Thus, it accumulates the change of air-pressure along its whole path and does not allow a direct imaging of side lobes within a sound field. However, for larger distances beyond near field this drawback has no significant consequences. Note that the depicted angle of the laser beam in Fig. 1 is overestimated due to image dimensions. During experiments the aspect ratio of LDV distance and scan area is much larger which allow imaging of the wave front easily. In contrast to LDV the area of detection of OM is much smaller as shown in Fig. 1(b) and in the order of only a few millimeters. This leads to very high spacial resolution but calls for additional scanning system for two-dimensional mapping of sound field properties.

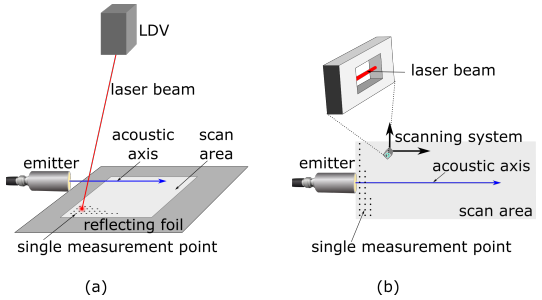

Figure 1: Working principle of scanning laser-doppler vibrometers (a) and optical microphones (b) for transducer characterization.

Results and Discussion

Characterization of a Thermo-Acoustic Emitter

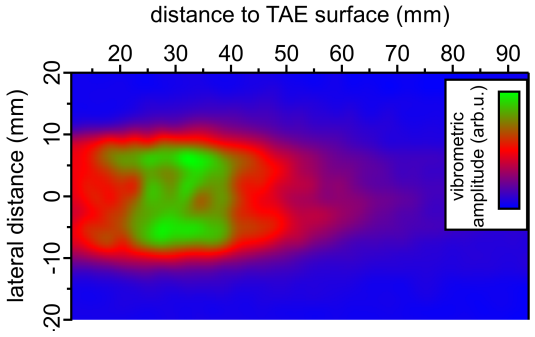

Figure 2: Vibrometric signal in front of the TAE.

As an example of a sound field measurement a home-built prototype of thermo-acoustic emitter (TAE) has been characterized. Such emitters can be used for further characterization of other transducers because they allow excitation with a short ultrasonic pulse. The active area of the TAE has a quadratic shape of $20 \times 20\,\mathrm{mm}^2$ and consists of a thin conductive layer (the exact material will not be mentioned here) on planar fused silica. The sound field measurement obtained with LDV is shown in Fig. 2.

Similar results of sound field measurements have been obtained using the OM but will not be further discussed. Note that those measurements are strongly influenced by additional noise of the scanning system (a stepper motor system have been used here) which easily lead to saturation of underlying objective signals.

Further analysis of the spectral composition of the data are shown in Fig. 3. Here FFT signals in dependence of

the distance along acoustic axis (see Fig. 2 at a lateral distance of 0 mm) are shown in a two-dimensional plot. The main frequency components are within a 10 and 120 kHz range. The signal at smaller distances below 35 mm increases which can be attributes to effects within the near-field length N which can be approximated using equation 1 where D is the aperture of the TAE and λ the wave length using 120 kHz. Above 35 mm an intensity drop is observed which is due to normal attenuation.

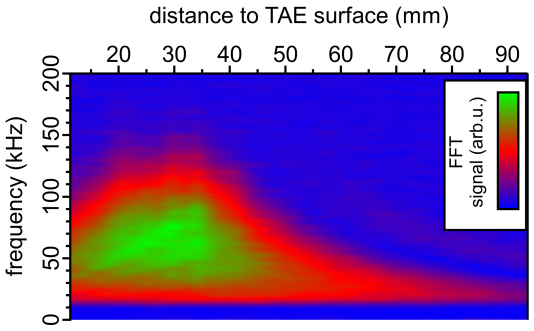

Figure 3: FFT-signals along acoustic axis in dependence of the distance.

$$N \approx D^2/4\lambda \qquad \text{(mm)} \qquad (1)$$

Normalization of the FFT spectra with respect to the maximum at each distance allows a closer look to the results as shown in Fig. 4. The frequency composition reveals quite interesting evolution with respect to the distance. First, the region above 35 mm will be discussed. Here the maximum shifts to lower frequencies. This can be explained by frequency-dependent attenuation of ultrasonic signals which increase with increasing frequencies as well. This influences the wave packet in time domain and elongates the pulse duration significantly (not shown here). Second, the region within the near-field length shows a shift of center frequency from approx. 50 kHz at a distance of 10 mm to 70 kHz at 30 mm which shifts back again at larger distances. Both observations have to taken into account by using this type of emitter for characterization of other ultrasonic transducers which will also be discussed in the receiver section below.

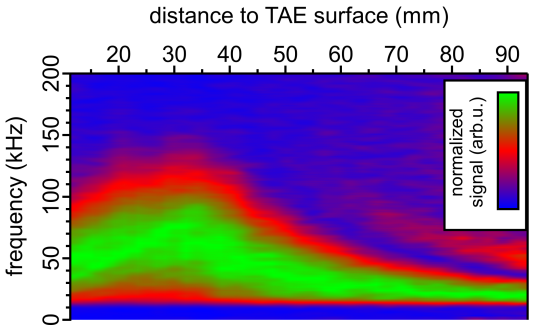

Figure 4: Same as fig. 3 but with normalized FFT signals at each distance point.

Direct comparison of LDV and OM spectra obtained at a distance of 40 mm is shown in Fig. 5. The dynamic range of both systems deviates. The LDV spans a range of only one order of magnitude (this is due actual settings, e.g. the sampling rate or the band filters and are not inherent limits of the system) whereas the OM reaches two orders of magnitude easily. However, both methods show significant differences. Obviously, the intensity distributions exhibit minor differences. The maximum obtained from OM measurement is located at a higher frequency of approx. 80 kHz instead of 50 kHz for LDV. Due to lower signal-to-noise ratio of actual LDV settings the progression at larger frequencies is not as obvious as for OM but the basic trend is similar.

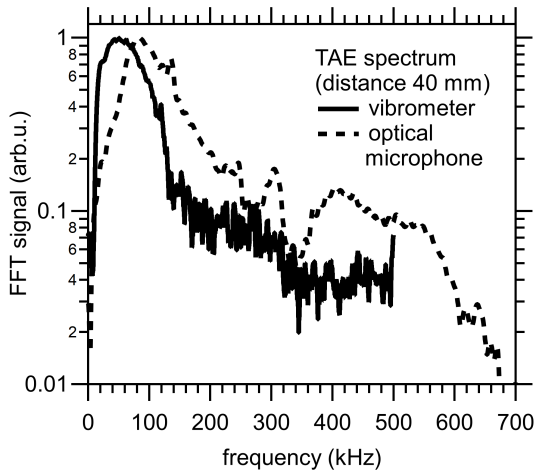

Figure 5: TAE spectra obtained from vibrometer and microphone measurements at a distance of 40 mm to TAE surface.

However, one important aspect has to be mentioned concerning the results of microphone measurements. As it can be seen in Fig. 5 the spectrum obtained from OM exhibit several distinct peaks, e.g. at 140, 250, and 300 kHz. Such peaks are not expected as a result of pulse generation of a TAE. Thus, the origin is most likely due to the setup itself. A closer look to the microphone head and its different inherent dimensions leads to possible explanation as depicted in Fig. 6. All occurring length scales can be converted into wave lengths and its corresponding frequencies as indicated in Fig. 6 as well. One can expect that those geometrical conditions lead to internal reflections which will cause artificial amplification of signal contributions due to resonance effects within the mentioned frequencies, half of those frequencies due to $\lambda/2$ effects, and its harmonics as well. Maybe the shifted position of the main maximum at approx. 80 kHz compared to LDV is already an indication of such resonance effects.

Characterization of Ultrasonic Emitters

Also air-coupled ultrasonic emitters can be characterized. The results can be used in terms of fundamental questions within research and development or even quality control in mass production processes. As an typical example we discuss results of broad-band prototype transducers which are based on piezo-fiber composites [6, 7]. The fiber-composites are resonators which mainly

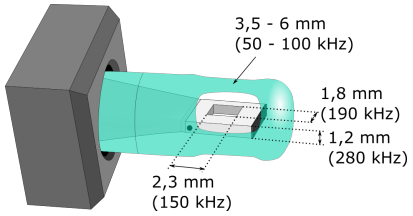

Figure 6: Head of the optical microphone. Inherent dimensions can be converted into possible resonance frequencies due to reflections. The upper 3.5 - 6 mm refer to various dimensions of the protection cap.

oscillate in thickness direction. Thus, the resonance frequency depends on thickness instead of diameter as well-known from conventional air-coupled ultrasonic transducers running at low frequencies. This enables to build up transducers with different frequencies but same apertures. This is a basic requirement to evaluate a characterization process where objective comparison of different transducers usually fails due to inherent differences of the transducer properties as frequency vs. aperture, i.e. size of active emitting area.

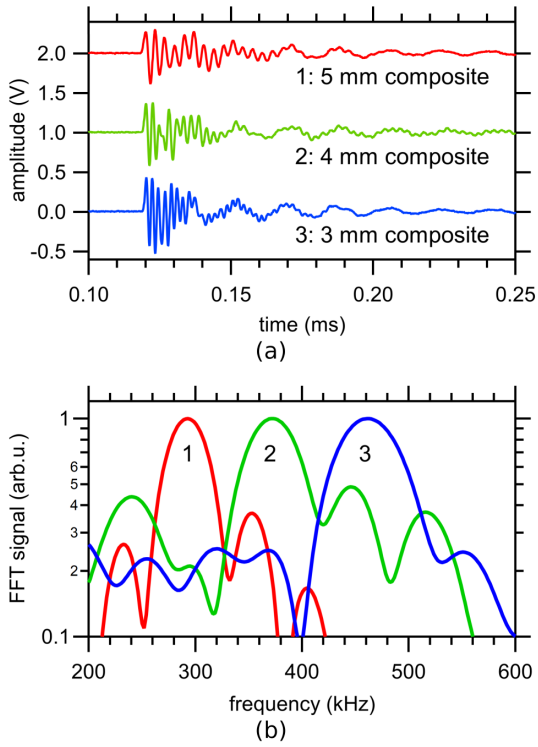

Figure 7: Raw data of the A-scans (a) and normalized FFT signals (b) obtained with OM of transducers with different fiber-composite thicknesses operated as emitters (distance 40 mm).

The results of impulse response are summarized in Fig. 7. For the determination of FFT spectra the first 8 oscillation cycles have been taken into account. The frequency shift in dependence of the composite thickness is nicely visible and the bandwidth of all transducers is in the order of 13%. According to this characterization the transducers have been excited with burst of 5 cycles and its corresponding resonance frequency (not shown here). According to calibration of the microphone the amplitudes of the signals can be directly converted into a sound pressure (measured in Pa) which lead to values of 410, 390, and 660 Pa for the 5, 4, and 3 mm thick composites (called '1', '2', and '3'), respectively. Note that we don't have to apply any frequency correction for determination of the sound pressure in case of emitter characterization. This becomes more complicated for receivers as it will be discussed in the following section.

Characterization of Ultrasonic Receivers

In this section the differences and particularities for the characterization of transducers which are running in receiving mode will be discussed. As well-known a single transducer can be utilized as an emitter or a receiver (assuming there are no special electric components which force a transducer to be an emitter or a receiver). The main difference of both operation modes is the resonance frequency for maximum amplitude (emitter) or sensitivity (receiver). As have been seen in the previous section resonance frequencies of the three transducers in emitting mode are 290, 370, and 470 kHz. For receivers it is expected that those values shift to higher frequencies. The corresponding spectra (obtained as mentioned below) are shown in Fig. 8(b) as dotted lines. The maximums are located at 350, 450, and 580 kHz, respectively.

$$S = U/p \qquad (\mu\mathrm{V/Pa}) \qquad (2)$$

For characterization of receivers we excite the transducer with a broad-band ultrasonic pulse as it is generated from TAE to be more or less independent of the excitation frequency (a probably so-called normalized source). This pulse leads to an electric response which can be used to define a receiving sensitivity S as given by Eq. 2 where U is the maximum voltage (peak-peak) achieved at the receiver and p the sound pressure of the TAE. In zero-order approximation one would measure the peak-peak amplitude of TAE signal as measured with OM, convert this signal to the sound pressure (compare black curve in Fig. 8(a) where we extract a sound pressure of 83 Pa) and gets the sensitivity of the transducer (expected voltage per incoming Pa). However, according to findings within the TAE section above the spectrum of TAE is rather complicated and depends on distance as well. One can expect that a receiver with a given frequency does not 'feel' the full amplitude of TAE due to its inherent filter effects (resonance frequency, matching layer, etc.). Ignoring those effects prevents an objective comparison of transducers especially if they run at different frequencies, i.e. a transducer at 100 kHz will lead to much higher signal because of the higher frequency components of TAE output in this frequency region.

We propose a frequency correction of the TAE signal as follows. Figure 8(b) shows the original spectrum of TAE as solid black line. Normalized receiving spectra of the transducers are shown as dotted lines. We approximate the main peak with a Gaussian fit and normalize TAE spectrum with the fitting curve. The results are shown in solid colored lines for the different transducers,

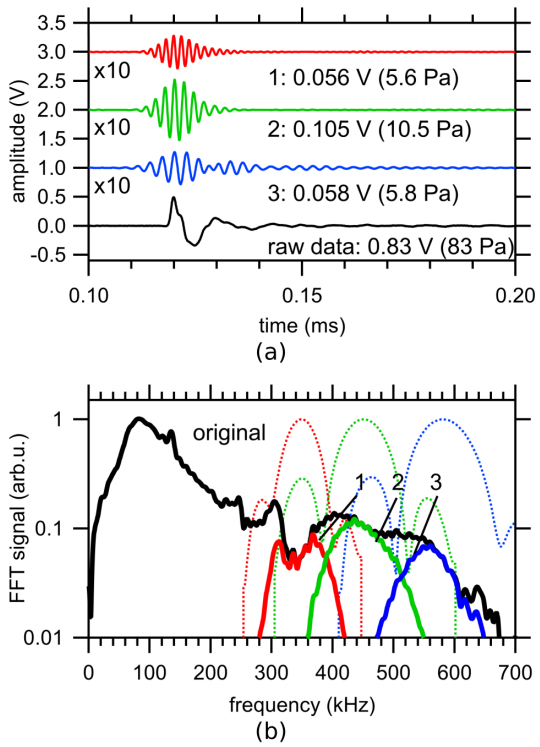

Figure 8: Original FFT signal (optical microphone) and signals after normalization to spectra of different receivers.

respectively. Afterward, we perform an inverse Fourier transformation of residual spectra and obtain signals in time domain as shown in Fig. 8(a). Note that corrected signals are multiplied by a factor of 10 for better reading. The amplitude of the signals is now assigned to the acoustically effective sound pressure for each individual transducer.

Table 1 summarizes all important results for zero-order approximation (top rows), frequency-corrected values (middle rows), and corresponding results of emitter characterization (bottom rows). It is expected that both modes (emitting and receiving) should reflect almost the same relative behavior, i.e. the highest emitting power should coincide with the highest receiving sensitivity as well and vice versa. This is not the case if we compare the relative performance (% values) of 'emitters' and the 'zero-order approximation'. The relative behavior of frequency-corrected data (middle) do fit much better to the expectation. Additionally note that the values of sensitivity are hardly underestimated in zero-order approximation. The corrected values exceed them by a factor of approx. 10 and are proposed to be more accurate. We also tested a combination of those transducers (emitter-receiver pairs) where the emitter output leads to receiver sensitivity values as obtained by the frequency-corrected method of TAE characterization.

Summary

We present a comparison of two optical methods for transducer characterization to enable quantitative statements about the performance of higher frequency air-coupled transducers. Both methods differs with respect to spacial resolution but lead to similar results. As examples emitting properties of TAE and broad-band transducers were discussed. The latter one were also used for receiver characterization were findings of part one lead to an interesting but necessary analysis for further data evaluation.

Table 1: Parameter of receiver and transmitter characterization obtained from OM data.

value	composite thickness 5 mm	4 mm	3 mm
	zero-order approximation		
f resonance (kHz)	350	450	580
signal intensity (V) (at 37 dB)	1.16	1.38	1.46
sensitivity (μV/Pa) (normalized)	197 (100%)	234 (119%)	248 (126%)
	frequency-corrected values		
TAE pressure (Pa)	5.6	10.5	5.8
sensitivity (μV/Pa) (normalized)	2920 (157%)	1860 (100%)	3580 (192%)
	emitter properties		
f resonance (kHz)	290	370	470
emitted pressure (Pa) (normalized)	410 (105%	390 (100%)	660 (169%)

References

[1] Edlén, J.A.: The refractive index of air, Metrologia 2 (1966), 71-80

[2] Stone, J.A., Zimmermann, J.H.:Index of Refraction of Air, URL: `https://emtoolbox.nist.gov`

[3] Polytec GmbH, Produktseite PSV-500-V, URL: `https://www.polytec.com/de/vibrometrie/produkte/full-field-vibrometer/psv-500-scanning-vibrometer/`

[4] XARION Laser Acoustics GmbH, Produktseite Eta250 Ultra, URL: `https://xarion.com/products/eta250-ultra`

[5] Jenderka, K.-V., *et al.*: Möglichkeiten zur räumlichen und zeitlichen Charakterisierung von Ultraschallfeldern in Luft mit scannender Laser-Doppler-Vibrometrie, DAGA 2015 Nürnberg (2015), 1086-1089

[6] Steinhausen, R. *et al.*: Zerstörungsfrei Prüfen mit Luftultraschall – Vom Wandler zum industriellen Prüfverfahren, Vortrag, DAGA 2019, URL: `http://2019.daga-tagung.de/programm/`

[7] Kiel, M. *et al.*: Quality Classification of Adhesive Bonds in Composite Structures by Single-sided Air-coupled Ultrasonic Testing, NDE of Aerospace Materials & Structures 2018, URL: `https://ndtlibrary.asnt.org/2018/`